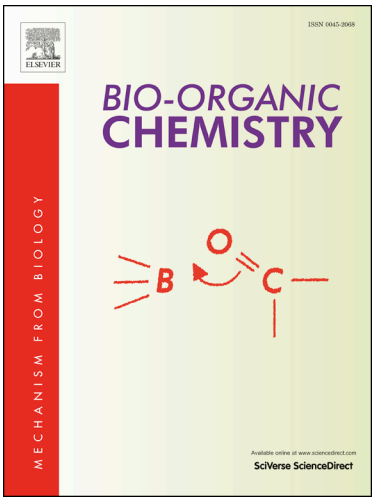

1,2,3-Triazole-based kojic acid analogs as potent tyrosinase inhibitors: Design, synthesis and biological evaluation

Morteza Ashooriha, Mehdi Khoshneviszadeh, Mahsima Khoshneviszadeh, Seyed Ershad Moradi, Alireza Rafiei, Mostafa Kardan, Saeed Emami

PII: S0045-2068(18)30861-7
DOI: https://doi.org/10.1016/j.bioorg.2018.10.069
Reference: YBIOO 2603

To appear in: *Bioorganic Chemistry*

Received Date: 10 August 2018
Revised Date: 30 October 2018
Accepted Date: 30 October 2018

Please cite this article as: M. Ashooriha, M. Khoshneviszadeh, M. Khoshneviszadeh, S. Ershad Moradi, A. Rafiei, M. Kardan, S. Emami, 1,2,3-Triazole-based kojic acid analogs as potent tyrosinase inhibitors: Design, synthesis and biological evaluation, *Bioorganic Chemistry* (2018), doi: https://doi.org/10.1016/j.bioorg.2018.10.069

1,2,3-Triazole-based kojic acid analogs as potent tyrosinase inhibitors: Design, synthesis and biological evaluation

Morteza Ashooriha [a], Mehdi Khoshneviszadeh [b,c], Mahsima Khoshneviszadeh [c], Seyed Ershad Moradi [d], Alireza Rafiei [e], Mostafa Kardan [e], Saeed Emami*[,f]

[a] *Department of Medicinal Chemistry, Student Research Committee, Faculty of Pharmacy, Mazandaran University of Medical Sciences, Sari, Iran*

[b] *Department of Medicinal Chemistry, Faculty of Pharmacy, Shiraz University of Medical Sciences, Shiraz, Iran*

[c] *Medicinal and Natural Products Chemistry Research Center, Shiraz University of Medical Sciences, Shiraz, Iran*

[d] *Pharmaceutical Sciences Research Center, Student Research Committee, Faculty of Pharmacy, Mazandaran University of Medical Sciences, Sari, Iran*

[e] *Department of Immunology and Molecular and Cell Biology Research Center, Hemoglobinopathy Institute, Faculty of Medicine, Mazandaran University of Medical Sciences, Sari, Iran*

[f] *Department of Medicinal Chemistry and Pharmaceutical Sciences Research Center, Faculty of Pharmacy, Mazandaran University of Medical Sciences, Sari, Iran*

Abstract: A series of kojic acid-derived compounds **6a-p** bearing aryloxymethyl-1*H*-1,2,3-triazol-1-yl moiety were designed by modifying primary alcoholic group of kojic acid as tyrosinase inhibitors. The target compounds **6a-p** were synthesized via click reaction. All compounds showed very potent anti-tyrosinase activity (IC_{50}s = 0.06-6.80 µM, being superior to reference drug, kojic acid. In particular, the naphthyloxy analogs **6o** and **6p** were found to be 31-155 times more potent than kojic acid. The metal-binding study of selected compound **6o** revealed that the prototype compound possesses metal-chelating ability, particularly with Cu^{2+} ions. The promising compounds **6o** and **6p** had acceptable safety profile as demonstrated by cytotoxicity assay against melanoma (B16) cell line and Human Foreskin Fibroblast (HFF) cells.

Keywords: Click reaction; hyperpigmentation; kojic acid; 1,2,3-triazole; tyrosinase inhibitor

***Correspondence:** Saeed Emami, Department of Medicinal Chemistry, Faculty of Pharmacy, Mazandaran University of Medical Sciences, Sari, Iran
E-mail: sdemami12@gmail.com; semami@mazums.ac.ir

1. Introduction

Melanin is a general name for wide range of natural pigments found in many species of living organisms and microorganisms such as animals, plants, fungi and bacteria. In mammals, melanin is synthesized in various part of their body like skin, eyes, hair and brain [1]. Various roles are attributed to melanin, but its significant function is protection of cells. For example, this molecule is pivotal for skin and eyes as a protective molecule against UV light [2]. Melanin is made and secreted by melanocytes in the basal layer of dermis. Despite the key role of melanin, its overproduction results in several hyperpigmentation disorders, such as freckles, senile lentigines and melasma [3]. Also, there are some evidences about correlation between neuromelanin and the pathogenesis of Parkinson's disease [4]. In agriculture industry, huge amount of vegetables and fruits are throwing away due to browning. This color change is also because of melanin overproduction [5]. Skin-whitening and depigmenting agents, which inhibit melanin formation, are used extensively in cosmetic products, hence they have great economic value in the cosmetic industry [6].

The process of melanin formation contains several steps including the hydroxylation of L-tyrosine to L-3-(3,4-dihydroxyphenyl)-alanine (L-DOPA) and also the subsequent oxidation of DOPA to dopaquinone. Dopaquinone is a reactive substance that can spontaneously polymerize to form melanin [7]. Two elementary oxidation reactions are rate-limiting steps of melanin production which catalyzed by tyrosinase enzyme [8]. Thus, this enzyme can be a suitable target to inhibit melanin formation. Tyrosinase is a metalloenzyme with coupled binuclear copper active site in which each of copper ion chelate with three histidine residue. This multifunctional enzyme catalyzes the oxidation of phenol and catechol by the coppers in presence of oxygen molecule [9, 10].

Many natural and synthetic compounds such as, arbutin, hydroquinone, azelaic acid and kojic acid (Fig. 1) have been reported as tyrosinase inhibitors [11,12]. However, few of them possess enough safety and potency in order to use in industry and medications. For example, there are some overwhelming evidences which indicate mutagenic and cytotoxic effects of hydroquinone against melanocytes. Furthermore, hydroquinone can cause local skin dryness or irritation, thereby leading to post-inflammatory hyperpigmentation [11]. Kojic acid is the most widely used compound among the skin-whitening agents in cosmetic products, but this compound has poor efficacy, insufficient stability and skin penetration. To overcome these drawbacks, higher concentration of kojic acid should be used, which results in incidence of

side effects [13,14]. Furthermore, kojic acid has been reported to have a high-sensitizing potential which can cause irritant contact dermatitis [15]. Thus, modification of kojic acid structure may be a new way to design of potent and safe tyrosinase inhibitors. Kojic acid-derived tyrosinase inhibitors have been reviewed comprehensively by us [14]. The esterification of alcoholic group and conversion of the 4-pyron structure into 4-pyridinone were the main modifications on kojic acid framework. For example, 3,4-methylenedioxy cinnamic acid ester of kojic acid has been reported as a potent tyrosinase inhibitor, being 14-fold more potent than parent compound, kojic acid [16]. Also, Ahn et al. described a kojic–trolox conjugate with more potent tyrosinase inhibitory activity compared to kojic acid [17]. It has been proven that alpha-hydroxy ketone structure of kojic acid has key role in tyrosinase inhibitory activity. By protecting of the enolic hydroxyl group, the tyrosinase inhibitory activity of kojic acid is also eliminated. Due to the structural similarity to tyrosine (native ligand), kojic acid can enter in the active site of tyrosinase and form a chelate complex with the copper ion [14]. In order to design new kojic acid analogs, we decide to reserve the main skeleton of kojic acid and substitute alcoholic hydroxyl group with a suitable substituent. For this purpose, we use click chemistry reaction and formation of 1,2,3-triazole ring. The click reaction has some outstanding features, including convenience in doing, stereo selectivity, and stability of the triazole in biologic conditions [18]. Thus we report here, the synthesis and biological evaluation of kojic acid analogs **6a-p** bearing aryloxymethyl-1*H*-1,2,3-triazol-1-yl moiety as potent tyrosinase inhibitors (Fig. 1).

2. Results and discussion

2.1. Chemistry

The kojic acid-derived compounds **6a-p** were synthesized in several steps as illustrated in Scheme 1. The commercially available starting material **1** was converted to chlorokojic **2** using thionyl chloride at room temperature [19]. The treatment of chlorokojic **2** with sodium azide in DMF afforded azidokojic derivative **3** under mild condition [20,21]. On the other hand, the phenolic compounds **4a-p** were reacted with propargyl bromide in the presence of K_2CO_3 in refluxing acetone to give the corresponding alkyne ethers **5a-p** [22]. Eventually, two key intermediates **3** and **5** were coupled by click reaction (azide–alkyne 1,3-dipolar cycloaddition) in a mixture of *tert*-BuOH: H_2O: THF (1:3:10) and catalytic amount of copper

sulphate pentahydrate and sodium ascorbate at room temperature to afford target compounds **6a-p**.

2.2. Tyrosinase inhibition

The effect of kojic acid derivatives **6a-p** on diphenolase activity was determined using mushroom tyrosinase enzyme in accordance to the reported protocol [23]. For this purpose, L-DOPA was used as the tyrosinase substrate in spectrophotometric assay. The obtained IC_{50} values of compounds **6a-p** against tyrosinase were reported in Table 1, in comparison with kojic acid as reference drug.

Generally, all compounds had significant inhibitory activity against tyrosinase, displaying IC_{50} values in the range of 0.06-6.80 µM. Their activities were higher than that of kojic acid (IC_{50} = 9.28 µM). The naphthyloxy derivatives **6o** and **6p** with IC_{50} values of 0.06 and 0.3 µM were found to be the most potent compounds. In particular, 1-naphthyloxy analog **6o** was 155 times more active than kojic acid.

From structure-activity relationship (SAR) point of view, the obtained results revealed that there is a strong relation between tyrosinase inhibition and the type of substituent on the aryloxy moiety of synthesized compounds. The comparison of unsubstituted phenoxy compound **6a** with halo-substituted derivatives **6b-f** indicated that the introduction of fluoro or chloro group on *para* or *meta* position increased the potency. In contract, substitution of bromo group on *para* position diminished the inhibitory activity. The differences between *para*- and *meta*-halo compounds were not significant. The presence of second chlorine atom in compound **6g** cannot improve the activity against tyrosinase.

The activity of 4-nitrophenoxy derivative **6i** was 2-fold superior to that of parent phenoxy compound **6a**. Thus, the presence of 4-nitro group has positive effect on activity. Furthermore, cyano and acetamido analogs (**6h** and **6j**) were less potent than **6a**. Also, hydroxymethyl and methoxy derivatives (**6k** and **6l**) were as potent as parent compound **4a**, indicating the tolerance of framework to $HOCH_2$ and CH_3O substituents for remaining intrinsic potency. Interestingly, the presence of 3,4,5-trimethoxy or 3,5-dimethyl substituents in compounds **6m** and **6n** resulted in greater potency.

Finally, annulation of benzene ring with phenoxy moiety of parent congener **6a** resulted in 1-naphthyloxy and 2-naphthyloxy analogs (**6o** and **6p**, respectively) with highest inhibitory activity against tyrosinase. However, the 1-naphthyloxy regioisomer **6o** was 5-fold more potent than 2-naphthyloxy derivative **6p**.

The mode of inhibition of the enzyme by the most potent derivative, **6o**, was determined by Lineweaver–Burk plot analysis. As shown in Fig. 2, the plots of 1/V versus 1/[S] gave a series of lines with slightly different slopes, intersecting in the lower left quadrant. The analysis showed that V_{max} and K_m values decreased in the presence of increasing concentrations of compound **6o**. With these results, it can presume that the type of inhibition for compound **6o** is a mixed, predominantly uncompetitive inhibition.

2.3. Antioxidant activity evaluation

As mentioned above (Introduction section), tyrosinase enzyme has monophenolase and diphenolase activities, catalyzing hydroxylation of monophenols to catechols and further oxidation to *o*-quinones using oxygen [24]. Probably, compounds with redox capability and antioxidant property may inhibit the oxidation process of substrates without interacting with the tyrosinase enzyme [25]. Thus, the potent inhibitors of tyrosinase reported in this communication were assessed for their possible free radical scavenging activity by using DPPH test.

The obtained results demonstrated that kojic acid-derived compounds **6a-p** possess high anti-tyrosinase activity with no DPPH free radical scavenging property. Thus, there is no evidence for indirect action of compounds on oxidization process of the tyrosinase enzyme and the observed inhibitions are related to the interaction with the enzyme.

2.4. Studies of metal-chelating properties

The metal-chelating properties of the promising compound **6o** toward biometals such as Cu^{2+}, Zn^{2+}, Fe^{2+} and Al^{3+} was studied by ultraviolet–visible (UV–Vis) spectrometry. The spectrum of **6o** was shown in Fig. 3A. When $CuSO_4$ was added, the absorption bands at 240 to 300 nm were enhanced. This enhancement for Cu^{2+} ion was greater than that of other ions. Additionally, the absorption in the range of 400 to 600 nm exhibited an enhancement, which

was same for all metal ions. These results indicated the formation of complexes between **6o** and tested metal ions.

To evaluate the stoichiometry of the **6o**–Cu^{2+} complex, titration experiment was performed using UV-vis spectrophotometry. The final concentration of **6o** was maintained at 50 μM, and the absorption spectra were recorded after addition of different concentrations of Cu^{2+}. The stoichiometry of the **6o**–Cu^{2+} complex was evaluated by determining the changes in absorbance at 249 nm, where the absorption band was enhanced (Fig. 3B). As shown in Fig. 4, the absorption increased with an increase in Cu^{2+} concentration and reached a plateau at Cu^{2+} molar ratio of 0.5, which indicated that the stoichiometry of **6o**–Cu^{2+} complex was 2:1.

2.5. Cytotoxicity evaluation

In order to verify the safety profile of kojic-derived compounds with potential tyrosinase inhibitory activity, the most potent compounds **6o** and **6p** were selected to test their cytotoxicity against B16 melanoma cell line and human foreskin fibroblast cells in comparison to reference drug kojic acid. As presented in Table 2, the IC_{50} values of compounds **6o** and **6p** against B16 melanoma cells were 65.0-67.5 μM, being less than that of kojic acid (IC_{50}= 144.4 μM). Furthermore, the test compounds exhibited cytotoxic activity against normal HFF cells at very high concentrations (IC_{50} values ≥138.7 μM). Since, the promising compounds **6o** and **6p** showed anti-tyrosinase activity at sub-micromolar concentrations; we could conclude that these compounds have good safety for potential application in the treatment of tyrosinase-related disorders.

2.6. Molecular docking study

Molecular docking was carried out to understand the mode of action and type of interactions between the most potent inhibitor **6o** and target enzyme, tyrosinase. As shown in Figure 5, the inhibitor adopts a folded U-shape conformation which is stabilized by coordination, hydrogen bonds and hydrophobic interactions. Importantly, the tyrosinase inhibition of compound **6o** apparently depended on the kojic acid residue of the molecule. Indeed, the 3-hydroxy-4-pyrone moiety of compound **6o** can locate into the active site pocket near the copper center. The 4-carbonyl group coordinates with copper ions, and also forms hydrogen

bond with His85. Furthermore, hydrogen bonds are generated between nitrogens of 1,2,3-triazole ring and His244. It was found the naphthyl moiety is involved in the hydrophobic interactions with Asn81, Cys83, and Thr324 (Figure 6). These findings confirm the potent inhibition of tyrosinase by compound **6o**, and agreed well with our hypothesis for design of prototype compounds **6** by inserting the 1,2,3-triazole ring and aryloxy moiety onto the kojic acid structure.

3. Conclusion

In order to find new potent tyrosinase inhibitors, we have designed and synthesized kojic acid-derived analogs **6a-p** bearing aryloxymethyl-1*H*-1,2,3-triazol-1-yl moiety via click reaction. The aryloxy part of the designed molecule was varied for molecular optimization and structure-activity relationships study. All compounds showed very potent anti-tyrosinase activity with IC_{50} values in the range of 0.06-6.80 μM, being superior to reference drug kojic acid. Certainly, the naphthyloxy analogs **6o** and **6p** were found to be 31-155 times more potent than kojic acid. The DPPH free radical scavenging assay showed that the synthesized compound had no significant antioxidant activity. Thus, there is no evidence for indirect action of compounds on oxidization process of the tyrosinase enzyme and the observed inhibitions are related to the interaction with the enzyme. The metal-binding study of selected compound **6o** revealed that the prototype compound possesses metal-chelating ability, particularly with Cu^{2+} ions. The promising compounds displayed acceptable safety profile as revealed by cytotoxicity assay against B16 melanoma cell line and Human Foreskin Fibroblast (HFF) cells. These properties make the prototype kojic acid-derived compound **6o** as a good candidate for development of potential agents for treatment of tyrosinase-related disorders in agriculture, food industry, and cosmetics.

4. Experimental

4.1. General

All starting materials, reagents and solvents were purchased from Sigma-Aldrich or Merck companies and were used as received without further purification. Chlorokojic acid (**2**) was synthesized from kojic acid in accordance with the literature method [19].

The completion of reaction was checked by TLC using precoated silica gel 60 F254 aluminum sheets. The UV lamp (254 nm) was used for TLC visualization and detection of spots. Melting points were determined in open capillary tubes using Bibby Stuart Scientific SMP3 apparatus (Stuart Scientific, Stone, UK) and are uncorrected. The IR spectra were recorded on a PerkinElmer FT-IR spectrophotometer using KBr disks. The NMR spectra were recorded using Bruker 400 or 500 spectrometers and chemical shifts are expressed as δ (ppm). The mass spectra of compounds were obtained using a HP 5937 Mass Selective Detector (Agilent Technologies, CA, USA). Elemental analyses for C, H and N were performed by using a CHN-O-rapid elemental analyzer (Heraeus GmbH, Hanau, Germany), and the results are within ± 0.4% of the theoretical values.

*4.2. Preparation of 2-(azidomethyl)-5-hydroxy-4H-pyran-4-one (**3**)*

The procedure of Atkinson et al. [26] was used with some modifications. A mixture of sodium azide (2.0 g, 30.77 mmol) in DMF (3 mL) was heated at 85 °C for 20 min. After cooling down to room temperature, chlorokojic (**2**, 1.5 g, 9.34 mmol) was added to the mixture and stirred overnight at ambient temperature. After completion of the reaction as monitored by TLC, the reaction was quenched by addition of water (5 mL). The precipitated crude product was separated by filtration, washed with water and dried in vacuum oven. The obtained brown solid was dissolved in tetrahydrofuran and filtered to obtain a clear solution. Then, the solvent was evaporated under reduced pressure to give pure compound **3**. Light brown solid; yield: 80%; m.p. 129-131 °C; ^{1}H NMR (500 MHz, DMSO-d_6) δ: 9.20 (s, 1H, OH), 8.07 (s, 1H, H-6 pyran), 6.42 (s, 1H, H-3 pyran), 4.32 (s, 2H, methylene).

*4.3. General procedure for the preparation of propargyl ethers **5a-p***

Propargyl bromide (1.2 mmol) was added to a mixture of phenolic compounds **4a-p** (1.0 mmol) and K_2CO_3 (1.2 mmol) in acetone (5 mL) and the mixture was stirred under reflux for 10 h. After completion of the reaction confirmed by TLC, the solid salts were separated by filtration and the filtrate was concentrated under reduced pressure to give corresponding pure propargyl ethers **5a-p**.

*4.4. General procedure for the preparation of 5-hydroxy-2-{(4-(aryloxymethyl)-1H-1,2,3-triazol-1-yl)methyl}-4H-pyran-4-ones (**6a-p**)*

Copper sulfate pentahydrate (30 mg, 10 mol%) and sodium ascorbate (95.1 mg, 40 mol%) were suspended in deoxygenated H_2O (3 mL) and stirred until the reaction mixture turned yellow. Then, azidokojic **3** (1.0 mmol) and alkyne **5** (1.2 mmol) were dissolved in THF–*tert*-butanol (10:1), and the solution was added to aqueous mixture containing in situ generated Cu(I). This reaction mixture was stirred for 3 h at ambient temperature. After completion of the reaction (checked by TLC), the solvent was removed and the residue was dissolved in hot THF. Then, this reaction mixture was filtered and evaporated to remove solvent under reduced pressure. The residue was washed with small amount of acetone or methanol and dried in vacuo to give desired compounds **6a-p**.

*4.4.1. 5-Hydroxy-2-((4-(phenoxymethyl)-1H-1,2,3-triazol-1-yl)methyl)-4H-pyran-4-one (**6a**)*

White solid; yield 83%; m.p. 161-164 °C; IR (KBr, cm^{-1}): 3246, 3112, 1626, 1500, 1458, 1391, 1219, 1033, 857, 756, 689, 482. ^{1}H NMR (500 MHz, DMSO-d_6) δ: 9.27 (br s, 1H, OH), 8.32 (s, 1H, H-6 pyran), 8.04 (s, 1H, triazole), 7.29 (dd, 2H, J = 8.6 and 7.5 Hz, H-3 and H-5 Ar), 7.02 (d, 2H, J = 8.6 Hz, H-2 and H-6 Ar), 6.94 (t, 1H, J = 7.3 Hz, H-4 Ar), 6.40 (s, 1H, H-3 pyran), 5.61 (s, 2H, OCH_2), 5.15 (s, 2H, NCH_2). ^{13}C NMR (125 MHz, DMSO-d_6) δ: 174.08, 161.04, 158.44, 146.51, 143.69, 140.50, 129.98, 125.84, 121.35, 115.14, 113.54, 61.31, 50.43. MS (m/z, %): 299 (M^+, 20), 178 (100), 151 (12), 125 (75), 112 (16), 94 (54), 77 (16), 67 (33), 51 (12). Anal. Calcd for $C_{15}H_{13}N_3O_4$: C, 60.20; H, 4.38; N, 14.04. Found: C, 60.22; H, 4.16; N, 14.00.

*4.4.2. 2-((4-((4-Fluorophenoxy)methyl)-1H-1,2,3-triazol-1-yl)methyl)-5-hydroxy-4H-pyran-4-one (**6b**)*

White solid; yield 85%; m.p. 128-131 °C; IR (KBr, cm^{-1}): 3265, 3112, 3068, 1638, 1506, 1452, 1381, 1276, 1030, 898, 838, 663, 465. ^{1}H NMR (500 MHz, DMSO-d_6) δ: 9.28 (br s, 1H, OH), 8.32 (s, 1H, H-6 pyran), 8.05 (s, 1H, triazole), 7.12 (t, 2H, J = 8.7 Hz, H-3 and H-5 Ar), 6.95-7.07 (m, 2H, H-2 and H-6 Ar), 6.39 (s, 1H, H-3 pyran), 5.60 (s, 2H, OCH_2), 5.13 (s, 2H, NCH_2). ^{13}C NMR (125 MHz, DMSO-d_6) δ: 174.08, 161.03, 157.15 (d, $J_{C,F}$= 234.7 Hz), 154.76, 146.52, 143.55, 140.49, 125.88, 116.55 (d, 2C, $J_{C,F}$= 8.0 Hz), 116.31 (d, 2C, $J_{C,F}$= 22.7 Hz), 113.52, 61.99, 50.44. MS (m/z, %): 317 (M^+, 20), 207 (25), 178 (100), 151 (16),

125 (87), 112 (83), 97 (25), 83 (41), 67 (40), 57 (43). Anal. Calcd for $C_{15}H_{12}FN_3O_4$: C, 56.78; H, 3.81; N, 13.24. Found: C, 56.96; H, 3.89; N, 13.11.

*4.4.3. 2-((4-((4-Chlorophenoxy)methyl)-1H-1,2,3-triazol-1-yl)methyl)-5-hydroxy-4H-pyran-4-one (**6c**)*

White solid; yield 73%; m.p. 158-160 °C; IR (KBr, cm^{-1}): 3260, 3095, 1615, 1500, 1386, 1224, 1024, 789, 690, 466. ^{1}H NMR (500 MHz, DMSO-d_6) δ: 9.32 (s, 1H, OH), 8.34 (s, 1H, H-6 pyran), 8.06 (s, 1H, triazole), 7.34 (d, 2H, J = 9.0 Hz, H-3 and H-5 Ar), 7.07 (d, 2H, J = 9.0 Hz, H-2 and H-6 Ar), 6.41 (s, 1H, H-3 pyran), 5.62 (s, 2H, OCH_2), 5.16 (s, 2H, NCH_2). ^{13}C NMR (125 MHz, DMSO-d_6) δ: 174.08, 160.99, 157.74, 146.52, 143.32, 140.49, 132.61, 125.96, 117.53, 113.55, 112.82, 61.67, 50.46. MS (m/z, %): 333 (M^+, 1), 207 (15), 149 (12), 125 (15), 111 (23), 97 (38), 85 (53), 71 (75), 57 (100). Anal. Calcd for $C_{15}H_{12}ClN_3O_4$: C, 53.99; H, 3.62; N, 12.59. Found: C, 54.17; H, 3.54; N, 12.80.

*4.4.4. 2-((4-((4-Bromophenoxy)methyl)-1H-1,2,3-triazol-1-yl)methyl)-5-hydroxy-4H-pyran-4-one (**6d**)*

White solid; yield 78%; m.p. 144-146 °C, IR (KBr, cm^{-1}): 3255, 3097, 1616, 1579, 1490, 1458, 1387, 1244, 1027, 914, 792, 756, 685, 596, 502. ^{1}H NMR (500 MHz, DMSO-d_6) δ: 9.32 (s, 1H, OH), 8.34 (s, 1H, H-6 pyran), 8.06 (s, 1H, triazole), 7.46 (d, 2H, J = 9.0 Hz, H-3 and H-5 Ar), 7.02 (d, 2H, J = 8.5 Hz, H-2 and H-6 Ar), 6.41 (s, 1H, H-3 pyran), 5.62 (s, 2H, OCH_2), 5.16 (s, 2H, NCH_2). MS (m/z, %): 352 (8), 280 (12), 207 (83), 170 (25), 144 (50), 131 (100), 112 (40), 103 (67), 71 (40), 55 (67). Anal. Calcd for $C_{15}H_{12}BrN_3O_4$: C, 47.64; H, 3.20; N, 11.11. Found: C, 47.53; H, 3.25; N, 10.97.

*4.4.5. 2-((4-((3-Fluorophenoxy)methyl)-1H-1,2,3-triazol-1-yl)methyl)-5-hydroxy-4H-pyran-4-one (**6e**)*

White solid; yield 81%; m.p. 177-178 °C; IR (KBr, cm^{-1}): 3166, 3110, 2936, 1633, 1501, 1381, 1425, 1276, 1032, 897, 676, 466. ^{1}H NMR (500 MHz, DMSO-d_6) δ: 9.28 (s, 1H, OH), 8.34 (s, 1H, H-6 pyran), 8.05 (s, 1H, triazole), 7.31 (dd, 1H, J = 15.9 and 7.3 Hz, H-4 Ar), 6.94 (dt, 1H, J = 11.4 and 2.4 Hz, H-2 Ar), 6.87 (dd, J = 8.4 and 2.3 Hz, H-6 Ar), 6.77 (dt, J = 8.8 and 2.3 Hz, H-5 Ar), 6.40 (s, 1H, H-3 pyran), 5.61 (s, 2H, OCH_2), 5.17 (s, 2H, NCH_2). MS (m/z, %): 317 (M^+, 21), 206 (20), 178 (100), 151 (15), 125 (85), 111 (40), 97 (30), 83 (35), 67 (45). Anal. Calcd for $C_{15}H_{12}FN_3O_4$: C, 56.78; H, 3.81; N, 13.24. Found: C, 56.76; H, 3.77; N, 13.31.

*4.4.6. 2-((4-((3-Chlorophenoxy)methyl)-1H-1,2,3-triazol-1-yl)methyl)-5-hydroxy-4H-pyran-4-one (**6f**)*

White solid; yield 79%; m.p. 135-136 °C; IR (KBr, cm^{-1}): 3258, 3126, 1636, 1460, 1388, 1229, 1004, 900, 860, 766, 680. ^{1}H NMR (500 MHz, DMSO-d_6) δ: 9.28 (s, 1H, OH), 8.33 (s, 1H, H-6 pyran), 8.04 (s, 1H, triazole), 7.31 (t, 1H, J = 8.2 Hz, H-5 Ar), 7.14 (dd, 1H, J = 2.0 and 2.2 Hz, H-2 Ar), 6.85-7.05 (m, 2H, H-4 and H-6 Ar), 6.40 (s, 1H, H-3 pyran), 5.61 (s, 2H, OCH_2), 5.19 (s, 2H, NCH_2). ^{13}C NMR (125 MHz, DMSO-d_6) δ: 174.08, 160.99, 159.39, 146.52, 143.23, 140.49, 134.21, 131.34, 126.02, 121.35, 115.26, 114.34, 113.56, 61.73, 50.46. MS (m/z, %): 333 (M^+, 13), 307 (8), 203 (66), 178 (70), 125 (68), 84 (50), 56 (100). Anal. Calcd for $C_{15}H_{12}ClN_3O_4$: C, 53.99; H, 3.62; N, 12.59. Found: C, 53.90; H, 3.73; N, 12.60.

*4.4.7. 2-((4-((2,4-Dichlorophenoxy)methyl)-1H-1,2,3-triazol-1-yl)methyl)-5-hydroxy-4H-pyran-4-one (**6g**)*

White solid; yield 85%; m.p. 150-151 °C; IR (KBr, cm^{-1}): 3300, 1640, 1476, 1381, 1262, 1217, 1112, 1059, 875, 804, 712. ^{1}H NMR (400 MHz, DMSO-d_6) δ: 9.32 (s, 1H, OH), 8.37 (s, 1H, H-6 pyran), 8.06 (s, 1H, triazole), 7.58 (br s, 1H, Ar), 7.40 (br s, 2H, Ar), 6.41 (s, 1H, H-3 pyran), 5.63 (s, 2H, OCH_2), 5.28 (s, 2H, NCH_2). ^{13}C NMR (125 MHz, DMSO-d_6) δ: 174.07, 160.98, 152.93, 146.52, 142.92, 140.47, 129.83, 128.51, 126.167, 125.40, 123.08, 116.22, 113.55, 62.78, 50.48. MS (m/z, %): 365 (2), 342 (7), 279 (14), 207 (72), 167 (31), 149 (100), 111 (17), 97 (65), 85 (35), 71 (55), 57 (86). Anal. Calcd for $C_{15}H_{11}Cl_2N_3O_4$: C, 48.94; H, 3.01; N, 11.41. Found: C, 49.13; H, 2.64; N, 11.66.

*4.4.8. 4-((1-((5-Hydroxy-4-oxo-4H-pyran-2-yl)methyl)-1H-1,2,3-triazol-4-yl)methoxy)benzonitrile (**6h**)*

White solid; yield 93%; m.p. 204-206 °C; IR (KBr, cm^{-1}): 3742, 3251, 3091, 2925, 2464, 1618, 1501, 1458, 1401, 1350, 1216, 1133, 1020, 947, 866, 763, 676, 508. ^{1}H NMR (500 MHz, DMSO-d_6) δ: 9.32 (s, 1H, OH), 8.38 (s, 1H, H-6 pyran), 8.06 (s, 1H, triazole), 7.79 (d, 2H, J = 8.5 Hz, H-3 and H-5 Ar), 7.22 (d, 2H, J = 8.5 Hz, H-2 and H-6 Ar), 6.41 (s, 1H, H-3 pyran), 5.62 (s, 2H, OCH_2), 5.28 (s, 2H, NCH_2). ^{13}C NMR (125 MHz, DMSO-d_6) δ: 174.08, 161.88, 160.96, 146.52, 142.86, 140.50, 134.67, 126.19, 119.53, 116.29, 113.57, 103.69, 61.80, 50.48. MS (m/z, %): 324 (M^+, 15), 206 (38), 178 (80), 125 (100), 97 (26), 67 (38). Anal. Calcd for $C_{16}H_{12}N_4O_4$: C, 59.26; H, 3.73; N, 17.28. Found: C, 59.42; H, 3.71; N, 17.14.

*4.4.9. 5-Hydroxy-2-((4-((4-nitrophenoxy)methyl)-1H-1,2,3-triazol-1-yl)methyl)-4H-pyran-4-one (**6i**)*

White solid; yield 71%; m.p. 212-214 °C; IR (KBr, cm^{-1}): 3271, 3123, 3073, 2936, 1643, 1512, 1386, 1276, 1134, 1024, 909, 887, 673. ^{1}H NMR (500 MHz, DMSO-d_6) δ: 9.33 (s, 1H, OH), 8.41 (s, 1H, H-6 pyran), 8.23 (d, 2H, J = 9.0 Hz, H-3 and H-5 Ar), 8.07 (s, 1H, triazole), 7.28 (d, 2H, J = 9.5 Hz, H-2 and H-6 Ar), 6.42 (s, 1H, H-3 pyran), 5.64 (s, 2H, OCH_2), 5.35 (s, 2H, NCH_2). MS (m/z, %): 344 (M^+, 4), 206 (42), 178 (80), 125 (100), 97 (27), 67 (38). Anal. Calcd for $C_{15}H_{12}N_4O_6$: C, 52.33; H, 3.51; N, 16.27. Found: C, 52.19; H, 3.43; N, 16.02.

*4.4.10. N-(4-((1-((5-Hydroxy-4-oxo-4H-pyran-2-yl)methyl)-1H-1,2,3-triazol-4-yl)methoxy)phenyl)acetamide (**6j**)*

White solid; yield 69%; m.p. 216-218 °C, IR (KBr, cm^{-1}): 3333, 3140, 3099, 1657, 1543, 1507, 1447, 1401, 1236, 1126, 1042, 957, 823, 672, 595, 520. ^{1}H NMR (500 MHz, DMSO-d_6) δ: 9.81 (s, 1H, NH), 9.32 (s, 1H, OH), 8.33 (s, 1H, H-6 pyran), 8.07 (s, 1H, triazole), 7.48 (d, 2H, J = 9.0 Hz, H-3 and H-5 Ar), 6.97 (d, 2H, J = 9.0 Hz, H-2 and H-6 Ar), 6.42 (s, 1H, H-3 pyran), 5.62 (s, 2H, OCH_2), 5.11 (s, 2H, NCH_2), 2.01 (s, 3H, CH_3). MS (m/z, %): 356 (M^+, 8), 232 (15), 178 (8), 151 (70), 125 (15), 109 (100), 80 (20), 53 (8). Anal. Calcd for $C_{17}H_{16}N_4O_5$: C, 57.30; H, 4.53; N, 15.72. Found: C, 57.11; H, 4.65; N, 15.71.

*4.4.11. 5-Hydroxy-2-((4-((4-(hydroxymethyl)phenoxy)methyl)-1H-1,2,3-triazol-1-yl)methyl)-4H-pyran-4-one (**6k**)*

White solid; yield 80%; m.p. 200-201 °C; IR (KBr, cm^{-1}): 3255, 3172, 2910, 1629, 1510, 1458, 1395, 1218, 1012, 758, 689. ^{1}H NMR (500 MHz, DMSO-d_6) δ: 9.33 (s, 1H, OH), 8.34 (s, 1H, H-6 pyran), 8.07 (s, 1H, triazole), 7.24 (d, 2H, J = 8.5 Hz, H-3 and H-5 Ar), 6.99 (d, 2H, J = 8.5 Hz, H-2 and H-6 Ar), 6.42 (s, 1H, H-3 pyran), 5.62 (s, 2H, OCH_2), 5.14 (s, 2H, NCH_2), 5.07 (br s, 1H, OH), 4.42 (s, 2H, CH_2OH). MS (m/z, %): 329 (M^+, 4), 311 (20), 207 (11), 178 (100), 151 (15), 125 (92), 107 (30), 67 (42). Anal. Calcd for $C_{16}H_{15}N_3O_5$: C, 58.36; H, 4.59; N, 12.76. Found: C, 58.40; H, 4.67; N, 12.53.

*4.4.12. 5-Hydroxy-2-((4-((4-methoxyphenoxy)methyl)-1H-1,2,3-triazol-1-yl)methyl)-4H-pyran-4-one (**6l**)*

White solid; yield 93%; m.p. 132-133 °C; IR (KBr, cm^{-1}): 3124, 1642, 1589, 1506, 1260, 1117, 1008, 789. ^{1}H NMR (500 MHz, DMSO-d_6) δ: 9.33 (br s, 1H, OH), 8.32 (s, 1H, H-6 pyran), 8.07 (s, 1H, triazole), 6.97 (d, 2H, J = 8.5 Hz, Ar), 6.87 (d, 2H, J = 9.0 Hz, Ar), 6.40 (s, 1H, H-3 pyran), 5.62 (s, 2H, OCH_2), 5.09 (s, 2H, NCH_2), 3.70 (s, 3H, OCH_3). MS (m/z, %): 329 (M^+, 61), 178 (38), 124 (100), 109 (70), 95 (30), 67 (23). Anal. Calcd for $C_{16}H_{15}N_3O_5$: C, 58.36; H, 4.59; N, 12.76. Found: C, 58.62; H, 4.62; N, 12.49.

*4.4.13. 5-Hydroxy-2-((4-((3,4,5-trimethoxyphenoxy)methyl)-1H-1,2,3-triazol-1-yl)methyl)-4H-pyran-4-one (**6m**)*

White solid; yield 78%; m.p. 146-147°C; IR (KBr, cm^{-1}): 3234, 1679, 1613, 1506, 1405, 1267, 1182, 1090, 838, 580, 482. ^{1}H NMR (500 MHz, DMSO-d_6) δ: 9.33 (br s, 1H, OH), 8.34 (s, 1H, H-6 pyran), 8.07 (s, 1H, triazole), 6.40 (s, H, H-3 pyran), 6.35 (s, 2H, H-2 and H-6 Ar), 5.62 (s, 2H, OCH_2), 5.14 (s, 2H, NCH_2), 3.75 (s, 6H, 2×CH_3O), 3.57 (s, 3H, CH_3O). ^{13}C NMR (125 MHz, DMSO-d_6) δ: 174.07, 161.10, 154.96, 153.79, 146.53, 143.71, 140.48, 125.79, 113.49, 93.32, 93.23, 61.77, 60.57, 56.33, 50.44. MS (m/z, %): 389 (M^+, 45), 374 (8), 184 (88), 169 (100), 144 (18), 125 (45), 97 (12), 69 (25). Anal. Calcd for $C_{18}H_{19}N_3O_7$: C, 55.53; H, 4.92; N, 10.79. Found: C, 55.31; H, 5.14; N, 11.02.

*4.4.14. 2-((4-((3,5-Dimethylphenoxy)methyl)-1H-1,2,3-triazol-1-yl)methyl)-5-hydroxy-4H-pyran-4-one (**6n**)*

White solid; yield 88%; m.p. 174-175°C; IR (KBr, cm^{-1}): 3250, 3091, 2927, 1618, 1501, 1401, 1350, 1269, 1219, 1133, 1020, 947, 857, 764, 675, 504. ^{1}H NMR (500 MHz, DMSO-d_6) δ: 9.32 (br s, 1H, OH), 8.31 (s, 1H, H-6 pyran), 8.06 (s, 1H, triazole), 6.64 (s, 2H, H-2 and H-6 Ar), 6.59 (s, 1H, H-4 Ar), 6.40 (s, 1H, H-3 pyran), 5.61 (s, 2H, OCH_2), 5.10 (s, 2H, NCH_2), 2.22 (s, 6H, 2×CH_3). ^{13}C NMR (125 MHz, DMSO-d_6) δ: 174.08, 161.08, 158.48, 146.52, 143.85, 140.48, 139.11, 125.72, 122.97, 113.50, 112.87, 113.50, 112.87, 61.23, 50.42, 21.51. MS (m/z, %): 327 (M^+, 3), 281 (8), 266 (8), 207 (30), 160 (16), 145 (100), 112 (60), 91 (45), 71 (67), 55 (90). Anal. Calcd for $C_{17}H_{17}N_3O_4$: C, 62.38; H, 5.23; N, 12.84. Found: C, 62.42; H, 5.19; N, 13.01.

*4.4.15. 5-Hydroxy-2-((4-((naphthalen-1-yloxy)methyl)-1H-1,2,3-triazol-1-yl)methyl)-4H-pyran-4-one (**6o**)*

White solid; yield 70%; m.p. 130-131 °C; IR (KBr, cm^{-1}): 3742, 3059, 1640, 1586, 1505, 1452, 1390, 1269, 1212, 1151, 1097, 971, 773, 578, 469. ^{1}H NMR (500 MHz, DMSO-d_6) δ:

9.33 (br s, 1H, OH), 8.47 (s, 1H, H-6 pyran), 8.12 (d, 1H, *J* = 8.0 Hz, H-8 naphthalene), 8.07 (s, 1H, triazole), 7.87 (d, 1H, *J* = 8.0 Hz, H-5 naphthalene), 7.45-7.54 (m, 3H, H-4, H-6 and H-7 naphthalene), 7.44 (t, 1H, *J* = 8.0 Hz, H-3 naphthalene), 7.18 (d, *J* = 7.5 Hz, H-2 naphthalene), 6.44 (s, 1H, H-3 pyran), 5.65 (s, 2H, OCH_2), 5.37 (s, 2H, NCH_2). ^{13}C NMR (500 MHz, DMSO-d_6) δ: 174.10, 161.06, 153.90, 146.53, 143.77, 140.52, 134.51, 127.94, 126.95, 126.59, 125.83, 125.36, 121.98, 120.86, 113.56, 106.33, 99.48, 62.08, 50.48. MS (m/z, %): 349 (M^+, 25), 178 (33), 144 (100), 115 (78), 97 (7), 67 (13). Anal. Calcd for $C_{19}H_{15}N_3O_4$: C, 65.32; H, 4.33; N, 12.03. Found: C, 65.18; H, 4.54; N, 11.87.

*4.4.16. 5-Hydroxy-2-((4-((naphthalen-2-yloxy)methyl)-1H-1,2,3-triazol-1-yl)methyl)-4H-pyran-4-one (**6p**)*

White solid; yield; 65%; m.p. 200-201 °C; IR (KBr, cm^{-1}): 3066, 1643, 1508, 1393, 1219, 1127, 1013, 830, 758, 475. ^1H NMR (500 MHz, DMSO-d_6) δ: 9.33 (s, 1H, OH), 8.40 (s, 1H, H-6 pyran), 8.07 (s, 1H, triazole), 7.84 (d, 2H, *J* = 9.0 Hz, H-5 and H-8 naphthalene), 7.82 (d, 1H, *J* = 8.0 Hz, H-4 naphthalene), 7.51 (d, 1H, *J* = 2.5 Hz, H-1 naphthalene), 7.47 (dt, 1H, *J* = 8.0 and 1.2 Hz, H-6 naphthalene), 7.36 (dt, 1H, *J* = 8.0 and 1.2 Hz, H-7 naphthalene), 7.20 (dd, 1H, *J* = 9.0 and 2.5 Hz, H-3 naphthalene), 6.44 (s, 1H, H-3 pyran), 5.63 (s, 2H, OCH_2), 5.29 (s, 2H, NCH_2). ^{13}C NMR (125 MHz, DMSO-d_6) δ: 174.10, 161.03, 156.34, 146.54, 143.57, 140.50, 134.64, 129.86, 129.09, 127.99, 127.22, 126.92, 125.97, 124.21, 119.11, 113.58, 107.71, 61.52, 50.48. MS (m/z, %): 349 (M^+, 27), 178 (15), 144 (100), 115 (61), 67 (11). Anal. Calcd for $C_{19}H_{15}N_3O_4$: C, 65.32; H, 4.33; N, 12.03. Found: C, 65.34; H, 4.26; N, 12.09.

4.5. Anti-tyrosinase assay

Mushroom tyrosinase (EC 1.14.18.1) (Sigma Chemical Co.) was subjected to enzymatic inhibition assay using L-DOPA as substrate [23]. The stock solutions of test compounds **6a-p** and kojic acid were prepared in DMSO (40 mM) and then diluted with phosphate buffer (pH= 6.8) to the required concentrations. Firstly, 10 μL of mushroom tyrosinase (0.5 mg/mL) was mixed with 160 μL of phosphate buffer (50 mM, pH= 6.8) in 96-well microplates, and then 10 μL of the test compound was added. After the mixture was pre-incubated at 28 °C for 20 min, 20 μL of L-DOPA solution (0.5 mM) was added to each well and dopachrome formation was monitored at 475 nm for 10 min. Each assay was conducted as triplicate and

DMSO without test compounds was used as control. The final concentration of DMSO in the test solution was less than 2.0%. The percent of inhibition was calculated according to the following equation:

Inhibition (%) =100 × ($Abs_{control}$ − $Abs_{compound}$)/$Abs_{control}$

The inhibitory effect of each compound was expressed as the required concentration for 50% inhibition of the enzyme activity (IC_{50}).

4.6. Kinetic analysis of the tyrosinase inhibition

A series of experiments were performed to determine the inhibition kinetics of compound **6o**. The inhibitor concentrations were: 0.25, 0.5, 1 µM. Substrate L-DOPA concentrations were 0, 0.1, 0.25, 0.75, and 1.5 mM in all kinetic studies. Pre-incubation and measurement time were the same as reported in the mushroom tyrosinase inhibition assay protocol. Maximum initial velocity was determined from initial linear portion of absorbance up to ten minutes after addition of L-DOPA with 1 min interval.

4.7. DPPH radical scavenging assay

The antioxidant activity of all synthesized compounds **6a-p** was determined by the diphenylpicrylhydrazine (DPPH) radical scavenging assay [27]. Various concentrations (1-100 µM) of the compounds **6a-p** in methanol were prepared in a 96-well microtiter plate. Then, the DPPH solution (5 µL, 1 mg/mL dissolved in methanol) was added to each well and the plate was shaken gently and left in the dark for 30 min. The absorbance of the solution in each well was measured at 517 nm by an ELISA reader (BioTek). The percentage of total radical scavenging activity was calculated based on the formula: (%) = 100× [($Abs_{(control)}$ − $Abs_{(sample)}$)/$Abs_{(control)}$], where $Abs_{(control)}$ = $Abs_{(DPPH)}$ + $Abs_{(solvent)}$.

4.8. Metal-chelating studies

The metal-chelating studies were performed with a JASCO V-630 spectrophotometer (Tokyo, Japan). The UV absorption spectra of compound **6o**, in the absence or presence of sulfate salts of Cu^{2+}, Al^{3+}, Fe^{2+}, and Zn^{2+} were recorded with wavelength ranging from 200 to

600 nm after incubating for 30 min at room temperature. The final volume of reaction mixture was 5 mL, and the final concentrations of tested compound and metals were 50 µM.

The stoichiometry of the **6o**–Cu^{2+} complex was determined from molar ratio method [28] by titrating the methanol solution of tested compound with ascending concentrations of $CuSO_4$. The final concentration of tested compound was 50 µM, and the final concentration of Cu^{2+} ranged from 5 to 50 µM. The UV spectra were recorded and treated by numerical subtraction of $CuSO_4$ and **6o** at corresponding concentrations. The absorbance of the absorption peak at 249 nm was plotted versus the mole fraction of Cu^{2+}. The breakpoint indicated the stoichiometry of the compound–Cu^{2+} complex.

4.9. Cytotoxicity determination (MTT assay)

B16 melanoma cell line and HFF (Human Foreskin Fibroblast) cells were obtained from Pasture Institute, Iran. The B16 cells (8000 cells/well) and HFF cells (10000 cells/well) were seeded in RPMI-1640 and DMEM mediums, respectively. The cultured medium was supplemented with 10% fetal bovine serum (FBS), 100 unit/ml of penicillin-G, 100 µg/ml of streptomycin in each well of a 96-well plate and incubated in a humidified incubator containing 5% CO_2 at 37 °C. The selected compounds **6o** and **6p**, and reference drug kojic acid were dissolved in dimethyl sulfoxide (DMSO) and then diluted with the desired medium to the different concentrations. The final concentration of DMSO was less than 1% in medium culture. The cultured cells were treated with various concentrations of compounds and incubated at 37 °C for 48 h. The culture medium was replaced with fresh medium containing MTT (3-(4,5-dimethylthiazol-2-yl)-2,5-diphenyltetrazolium bromide) with a final concentration of 0.5 mg/mL, and incubated for further 4 h. Then, the medium containing MTT was removed and the remaining formazan crystals were dissolved in DMSO. The absorbance of each well was recorded in an ELISA reader (BioTek) at 570 nm [23]. Two independent experiments in triplicate were carried out for determination of cell viability for each compound. The IC_{50} values were calculated from concentration–viability rate curves using Prism 6, GraphPad Software and expressed as means ± SD.

4.10. Docking study

The X-ray structure of mushroom tyrosinase with the cognate ligand tropolone was extracted from the Protein Data Bank (PDB code 2Y9X). Before docking, some corrections should be made, such as, the removal of water molecules, the addition of Gasteiger charges and polar hydrogens in enzyme molecule by using the AutoDock tools (ADT) 1.5.4 package. The ligand was constructed and energy minimized using MOPAC Chem3D Ultra 8.0.3. Finally, ADT, Discovery Studio, ViewerLite, and LIGPLOT plus were used to evaluate the docking of ligand in the active site of tyrosinase and 2D and 3D visualization.

Acknowledgments

This work was supported by a grant (No. 2781) from the Research Council of Mazandaran University of Medical Sciences, Sari, Iran. This work was related to the Ph.D. thesis of MA (Faculty of Pharmacy, Mazandaran University of Medical Sciences).

References

[1] S. Piña-Oviedo, C. Ortiz-Hidalgo, A.G. Ayala, Human colors-the rainbow garden of pathology: what gives normal and pathologic tissues their color? Arch. Pathol. Lab. Med. 141 (2017) 445–462.

[2] D. Mohania, S. Chandel, P. Kumar, V. Verma, K. Digvijay, D. Tripathi, K. Choudhury, S.K. Mitten, D. Shah, Ultraviolet radiations: skin defense-damage mechanism. Adv. Exp. Med. Biol. 996 (2017) 71–87.

[3] S. Kumari, S.T.G. Thng, N.K. Verma, H.K. Gautam, Melanogenesis inhibitors. Acta Derm. Venereol. 2018, doi: 10.2340/00015555-3002.

[4] A. Bose, G.A. Petsko, D. Eliezer, Parkinson's disease and melanoma: co-occurrence and mechanisms. J. Parkinsons Dis. 8 (2018) 385–398.

[5] F. Taranto, A. Pasqualone, G. Mangini, P. Tripodi, M.M. Miazzi, S. Pavan, C. Montemurro, Polyphenol oxidases in crops: biochemical, physiological and genetic aspects. Int. J. Mol. Sci. 18 (2017) pii: E377. doi: 10.3390/ijms18020377.

[6] T. Pillaiyar, M. Manickam, V. Namasivayam, Skin whitening agents: medicinal chemistry perspective of tyrosinase inhibitors. J. Enzyme Inhib. Med. Chem. 32 (2017) 403–425.

[7] F. Solano, On the metal cofactor in the tyrosinase family. Int. J. Mol. Sci. 19 (2018) pii: E633. doi: 10.3390/ijms19020633.

[8] Á. Sánchez-Ferrer, J.N. Rodríguez-López, F. García-Cánovas, F. García-Carmona, Tyrosinase: a comprehensive review of its mechanism, Biochim. Biophys. Acta (BBA)-Protein Struct. Mol. Enzymol. 1247 (1995) 1–11.

[9] W. Xie, H. Zhang, J. He, J. Zhang, Q. Yu, C. Luo, S. Li, Synthesis and biological evaluation of novel hydroxybenzaldehyde-based kojic acid analogues as inhibitors of mushroom tyrosinase. Bioorg. Med. Chem. Lett. 27 (2017) 530–532.

[10] S. Radhakrishnan, R. Shimmon, C. Conn, A. Baker, Integrated kinetic studies and computational analysis on naphthyl chalcones as mushroom tyrosinase inhibitors, Bioorg. Med. Chem. Lett. 25 (2015) 4085–4091.

[11] M.R. Loizzo, R. Tundis, F. Menichini, Natural and synthetic tyrosinase inhibitors as antibrowning agents: an update, Compr. Rev. Food Sci. Food Saf. 11 (2012) 378–398.

[12] S. Emami, S.J. Hosseinimehr, K. Shahrbandi, A.A. Enayati, Z. Esmaeeli, Synthesis and evaluation of 2(3*H*)-thiazole thiones as tyrosinase inhibitors. Arch. Pharm. 345 (2012) 629–637.

[13] W.-C. Chen, T.-S. Tseng, N.-W. Hsiao, Y.-L. Lin, Z.-H. Wen, C.-C. Tsai, Y.-C. Lee, H.-H. Lin, K.-C. Tsai, Discovery of highly potent tyrosinase inhibitor, T1, with significant anti-melanogenesis ability by zebrafish in vivo assay and computational molecular modeling, Sci. Rep. 5 (2015) 7995.

[14] S.M. Hashemi, S. Emami, Kojic acid-derived tyrosinase inhibitors: synthesis and bioactivity, Pharmaceutical and Biomedical Research 1 (2015) 1–17

[15] T. Piamphongsant, Treatment of melasma: a review with personal experience. Int. J. Dermatol. 37 (1998) 897–903.

[16] H.-S. Rho, M.-I. Goh, J.-K. Lee, S.-M. Ahn, J.-H. Yeon, D.-S. Yoo, D.-H. Kim, H.-G. Kim, J.-Y. Cho, Ester derivatives of kojic acid and polyphenols containing adamantane

moiety with tyrosinase inhibitory and anti-inflammatory properties, Bull. Korean Chem. Soc. 32 (2011) 1411–1414.

[17] S.M. Ahn, H.S. Rho, H.S. Baek, Y.H. Joo, Y.D. Hong, S.S. Shin, Y.-H. Park, S.N. Park, Inhibitory activity of novel kojic acid derivative containing trolox moiety on melanogenesis, Bioorg. Med. Chem. Lett. 21 (2011) 7466–7469.

[18] P. Thirumurugan, D. Matosiuk, K. Jozwiak, Click chemistry for drug development and diverse chemical--biology applications, Chem. Rev. 113 (2013) 4905–4979.

[19] S. Emami, E. Ghafouri, M.A. Faramarzi, N. Samadi, H. Irannejad, A. Foroumadi, Mannich bases of 7-piperazinylquinolones and kojic acid derivatives: Synthesis, in vitro antibacterial activity and in silico study, Eur. J. Med. Chem. 68 (2013) 185–191.

[20] J.A. Durden, H.A. Stansbury, W.H. Catlette, The reaction of azidoörganic compounds with acetylenes., J. Chem. Eng. Data. 9 (1964) 228–232.

[21] S.M. Meier, M. Novak, W. Kandioller, M.A. Jakupec, V.B. Arion, N. Metzler-Nolte, B.K. Keppler, C.G. Hartinger, Identification of the structural determinants for anticancer activity of a ruthenium arene peptide conjugate, Chem. Eur. J. 19 (2013) 9297–9307.

[22] A.H. Banday, S.A. Shameem, B.D. Gupta, H.M.S. Kumar, D-ring substituted 1, 2, 3-triazolyl 20-keto pregnenanes as potential anticancer agents: Synthesis and biological evaluation, Steroids 75 (2010) 801–804.

[23] Y.S. Lee, J.H. Park, M.H. Kim, S.H. Seo, H.J. Kim, Synthesis of tyrosinase inhibitory kojic acid derivative, Arch. Pharm. Chem. Life Sci. 339 (2006) 111–114.

[24] J.R. Whitaker, Polyphenol oxidase. In: Food Enzymes, Structure and Mechanism (Ed.: D. W. S. Wong), Chapman & Hall, New York 1995, pp. 271–307.

[25] S.Y. Seo, V.K. Sharma, N. Sharma, Mushroom tyrosinase: recent prospects. J. Agric. Food Chem. 51 (2003) 2837–2853.

[26] J.G. Atkinson, Y. Girard, J. Rokach, C.S. Rooney, C.S. McFarlane, A. Rackham, N.N. Share, Kojic amine--a novel gamma-aminobutyric acid analogue. J. Med. Chem. 22 (1979) 99–106.

[27] K.-H. Lee, F.H.A. Aziz, A. Syahida, F. Abas, K. Shaari, D.A. Israf, N.H. Lajis,

Synthesis and biological evaluation of curcumin-like diarylpentanoid analogues for anti-inflammatory, antioxidant and anti-tyrosinase activities. Eur. J. Med. Chem. 44 (2009) 3195–3200.

[28] A.S. Jr. Meyer, G. H. Ayres, The mole ratio method for spectrophotometric determination of complexes in solution. J. Am. Chem. Soc. 79 (1957) 49–53.

Captions:

Figure 1. Structures of well-known tyrosinase inhibitors and designed compounds.

Figure 2. Lineweaver-Burk plots for inhibition of selected compound **6o** on mushroom tyrosinase for the oxidation of L-DOPA.

Figure 3. A) The UV spectrum of compound **6o** (50 μM, in methanol) alone or in the presence of sulfate salt of Cu^{2+}, Fe^{2+}, Zn^{2+} and Al^{3+} (50 μM, in methanol). B) UV spectrum of compound **6o** (final concentration was 50 μM) alone or in the presence of Cu(II) (the final concentration of Cu^{2+} ranged from 0 μM to 50 μM).

Figure 4. Determination of the stoichiometry of **6o**-Cu^{2+} complex by using molar ratio method through titration the methanol solution of compound **6o** with ascending amounts of $CuSO_4$. The final concentration of tested compound was 50 μM, and the final concentration of Cu^{2+} ranged from 5 to 50 μM.

Figure 5. 3D presentations for binding mode of compound **6o** into the binding site of tyrosinase.

Figure 6. 2D representation for the interactions of compound **6o** with the residues in the active site of tyrosinase, visualized by LIGPLOT.

Scheme 1. Synthesis of compounds **6a-p**.

Table 1. Tyrosinase inhibitory activity of compounds **6a-p**.

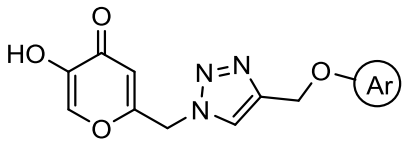

Compound	Ar	IC_{50} (μM)
6a		1.33 ± 0.18
6b	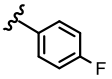	0.88 ± 0.03
6c	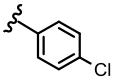	0.69 ± 0.091
6d	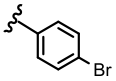	6.80 ± 0.42
6e	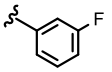	1.07 ± 0.16
6f	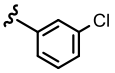	0.99 ± 0.15
6g	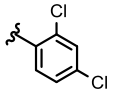	1.12 ± 0.18
6h	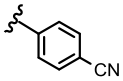	6.29 ± 1.28
6i	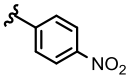	0.52 ± 0.13
6j	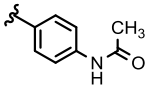	2.64 ± 0.13
6k	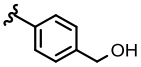	1.32 ± 0.15
6l	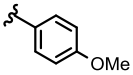	1.24 ± 0.25
6m	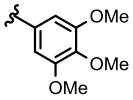	0.87 ± 0.17
6n	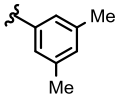	0.74 ± 0.08
6o	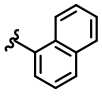	0.06 ± 0.02
6p	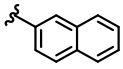	0.30 ± 0.14
Kojic acid	-	9.28 ± 1.12

Table 2. Cytotoxic activity (IC_{50}, μM) of selected compounds **6o**, **6p** and kojic acid against melanoma (B16) and Human Foreskin Fibroblast (HFF) cell lines.

Compound	Structure	B16	HFF
6o	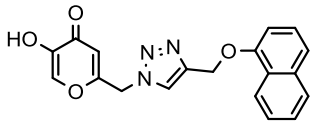	65.0 ± 1.1	138.7 ± 1.5
6p	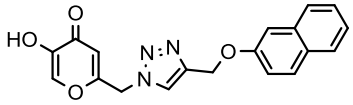	67.5 ± 0.8	149.5 ± 0.9
Kojic acid	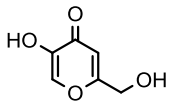	144.4 ± 2.3	>150

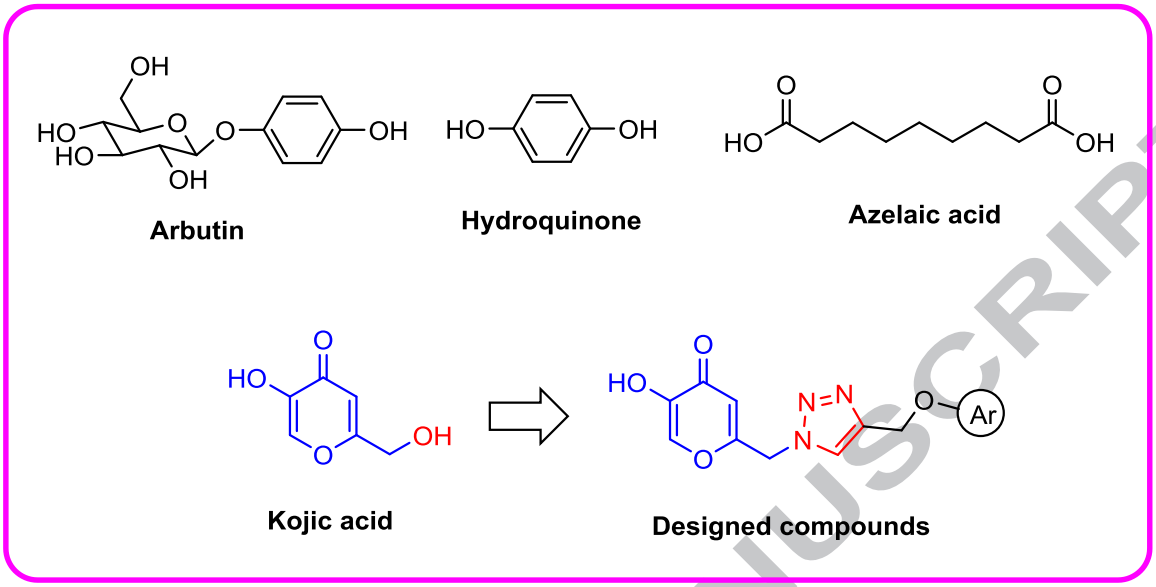

Figure 1. Structures of well-known tyrosinase inhibitors and designed compounds.

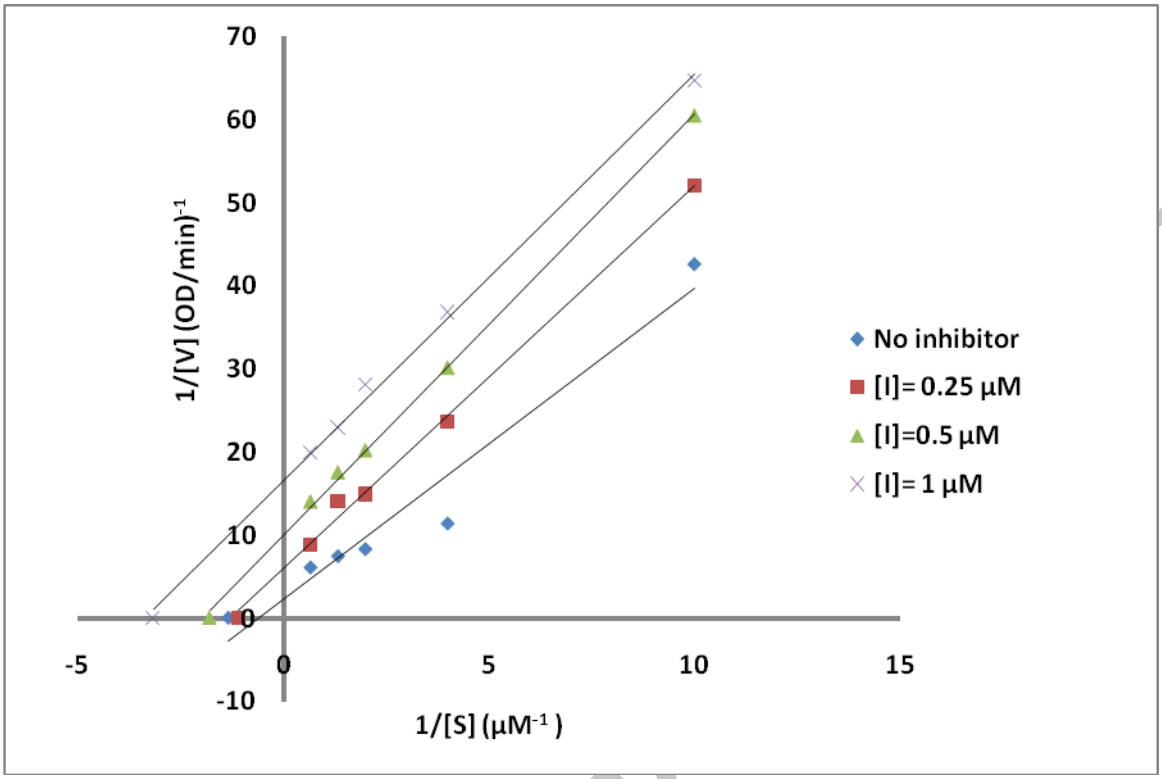

Figure 2. Lineweaver-Burk plots for inhibition of selected compound **6o** on mushroom tyrosinase for the oxidation of L-DOPA.

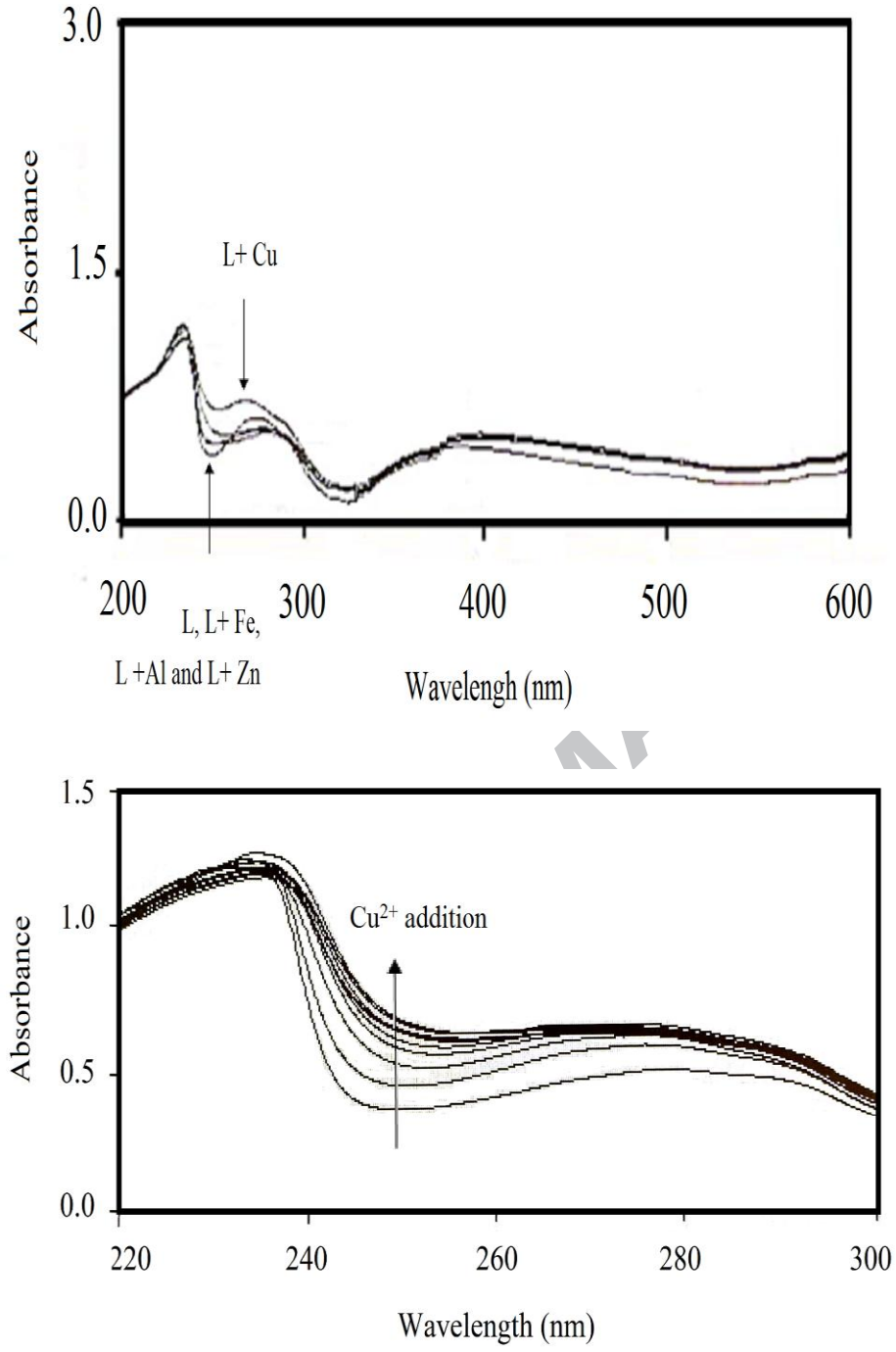

Figure 3. A) The UV spectrum of compound **6o** (50 µM, in methanol) alone or in the presence of sulfate salt of Cu^{2+}, Fe^{2+}, Zn^{2+} and Al^{3+} (50 µM, in methanol). B) UV spectrum of compound **6o** (final concentration was 50 µM) alone or in the presence of Cu(II) (the final concentration of Cu^{2+} ranged from 0 µM to 50 µM).

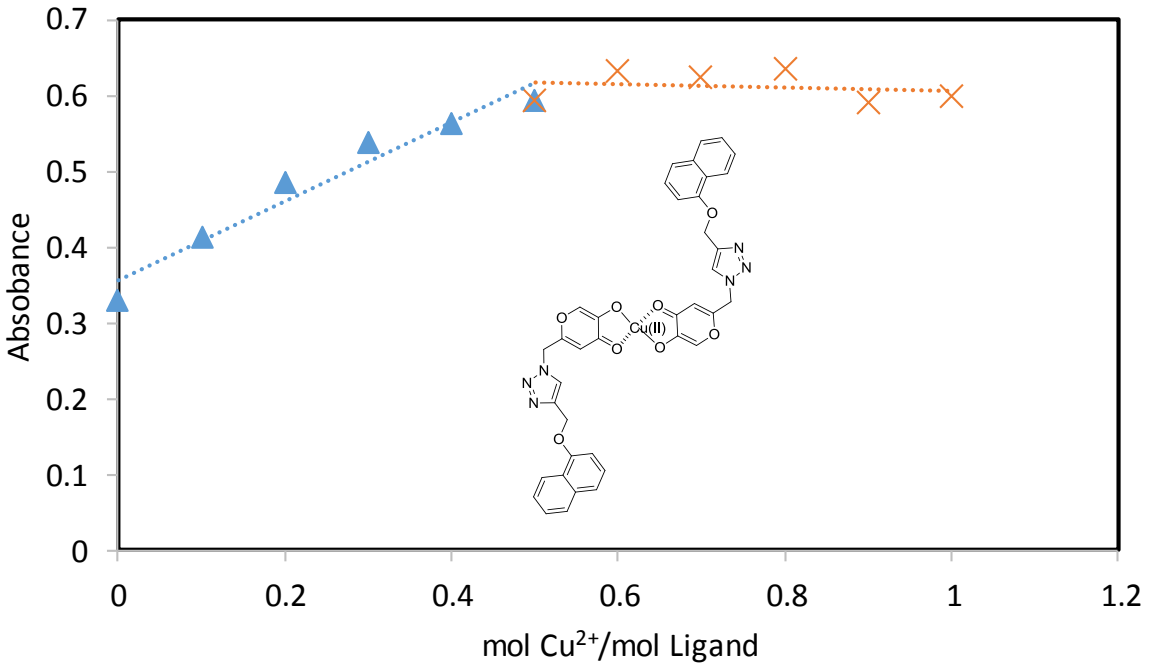

Figure 4. Determination of the stoichiometry of **6o**-Cu^{2+} complex by using molar ratio method through titration the methanol solution of compound **6o** with ascending amount of $CuSO_4$. The final concentration of tested compound was 50 μM, and the final concentration of Cu^{2+} ranged from 5 to 50 μM.

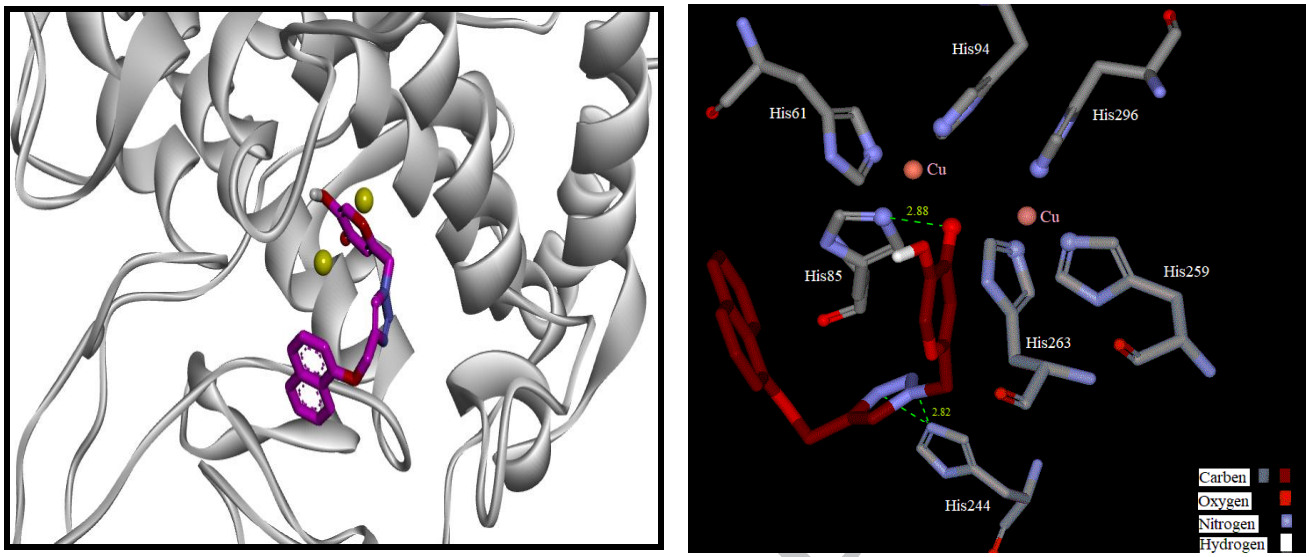

Figure 5. 3D presentations for binding mode of compound **6o** into the binding site of tyrosinase.

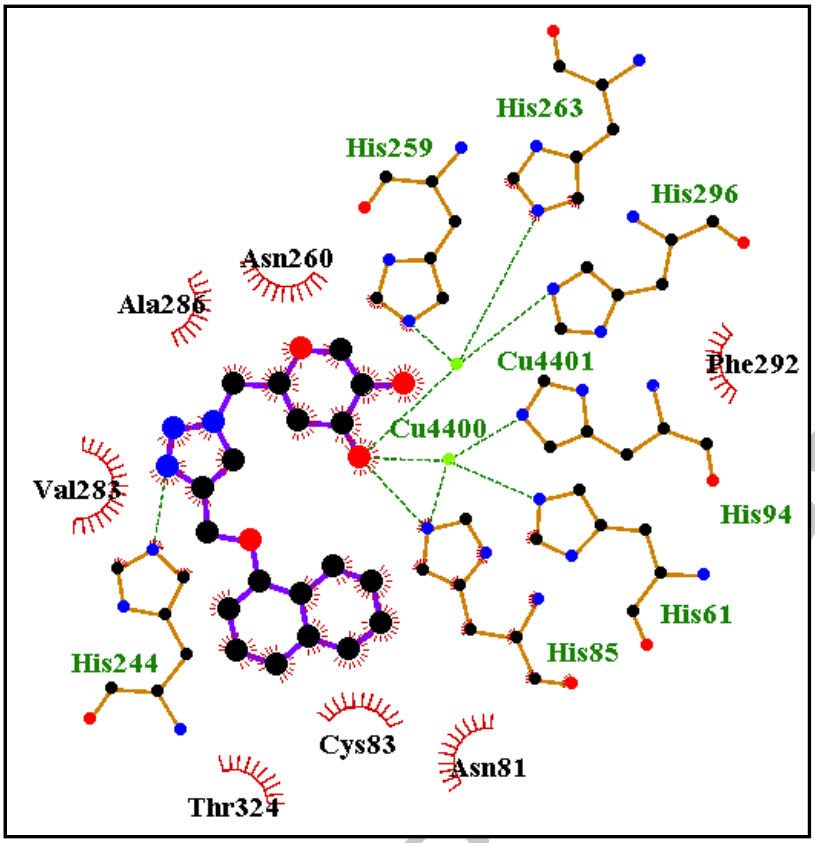

Figure 6. 2D representation for the interactions of compound **6o** with the residues in the active site of tyrosinase, visualized by LIGPLOT.

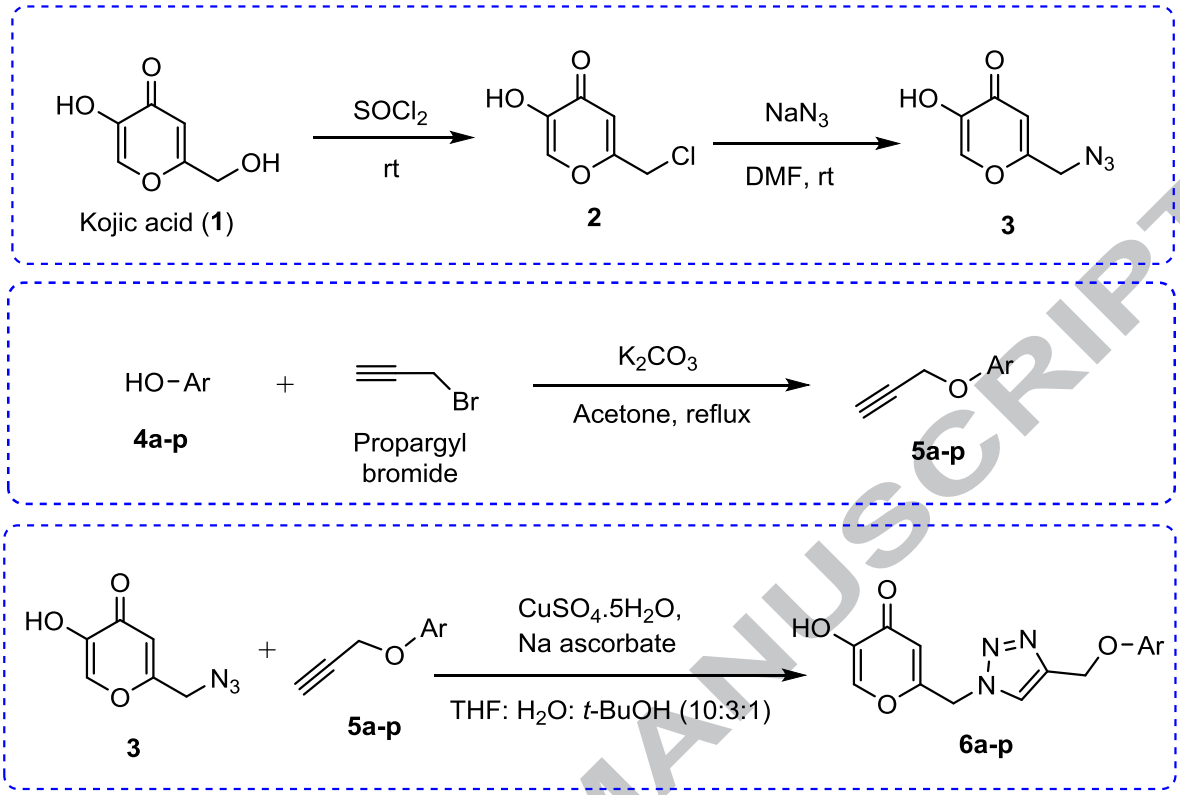

Scheme 1. Synthesis of compounds **6a-p**.

Graphical Abstract

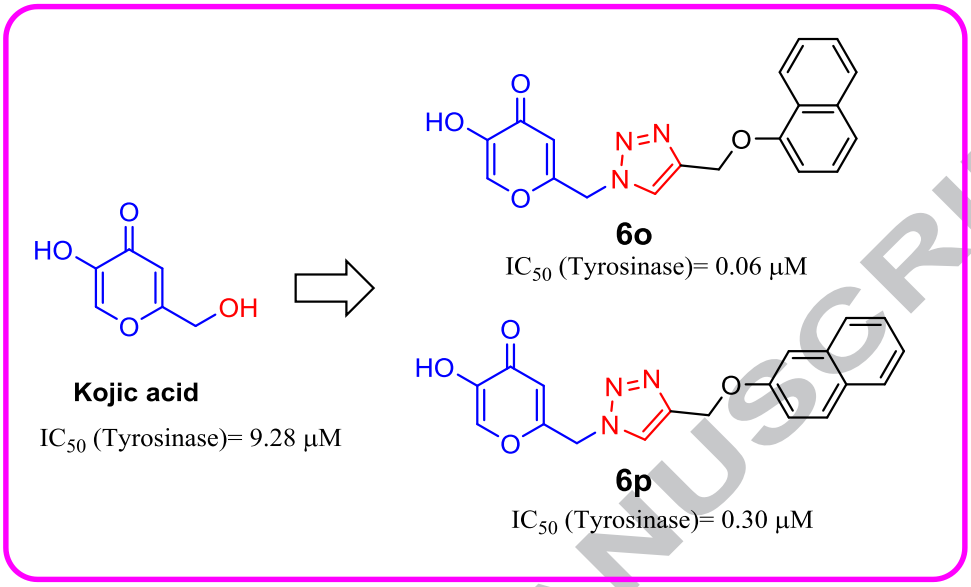

Highlights

- The alcoholic group of kojic acid was modified to aryloxymethyl-1,2,3-triazolyl moiety.
- The target compounds **6a-p** were synthesized via click reaction.
- All compounds showed very potent anti-tyrosinase activity greater than kojic acid.
- Naphthyloxy analogs **6o** and **6p** were the most potent compounds (IC_{50}s = 0.06-0.30 µM).
- **6o** and **6p** affect viability of B16 and HFF cells only at high concentrations.